

The Galactic Lithium Evolution Revisited

Donatella Romano^{1,2}, Francesca Matteucci^{3,1}, Paolo Molaro², Piercarlo Bonifacio²

¹ SISSA/ISAS, Via Beirut, 2-4, 34014 Trieste, Italy

² Osservatorio Astronomico di Trieste, Via G.B. Tiepolo, 11, 34131 Trieste, Italy

³ Dipartimento di Astronomia, Università di Trieste, Via G.B. Tiepolo, 11, 34131 Trieste, Italy

November 13, 2017

Abstract. The evolution of the ${}^7\text{Li}$ abundance in the Galaxy has been computed by means of the two-infall model of Galactic chemical evolution. We took into account several stellar ${}^7\text{Li}$ sources: novae, massive AGB stars, C-stars and Type II SNe. In particular, we adopted new theoretical yields for novae. We also took into account the ${}^7\text{Li}$ production from GCRs. In particular, the absolute yields of ${}^7\text{Li}$, as suggested by a recent reevaluation of the contribution of GCR spallation to the ${}^7\text{Li}$ abundance, have been adopted.

We compared our theoretical predictions for the evolution of ${}^7\text{Li}$ abundance in the solar neighborhood with a new compilation of data, where we identified the population membership of the stars on a kinematical basis. A critical analysis of extant observations revealed a possible extension of the Li plateau towards higher metallicities (up to $[\text{Fe}/\text{H}] \sim -0.5$ or even -0.3) with a steep rise afterwards.

We conclude that 1) the ${}^7\text{Li}$ contribution from novae is required in order to reproduce the shape of the growth of $A(\text{Li})$ versus $[\text{Fe}/\text{H}]$, 2) the contribution from Type II SNe should be lowered by at least a factor of two, and 3) the ${}^7\text{Li}$ production from GCRs is probably more important than previously estimated, in particular at high metallicities: by taking into account GCR nucleosynthesis we noticeably improved the predictions on the ${}^7\text{Li}$ abundance in the presolar nebula and at the present time as inferred from measures in meteorites and T Tauri stars, respectively. We also predicted a lower limit for the present time ${}^7\text{Li}$ abundance expected in the bulge, a prediction which might be tested by future observations.

Key words: Galaxy: chemical evolution – stars: evolution, abundances – cosmic rays – ISM: abundances plot

Send offprint requests to: D. Romano, e-mail: romano@sissa.it

1. Introduction

Since Spite & Spite (1982) discovered that the oldest, warm halo dwarfs in the Galaxy all show almost the same ${}^7\text{Li}$ abundance, several papers have appeared in the literature supporting their initial interpretation that this is the primordial abundance of ${}^7\text{Li}$ (Spite, Maillard & Spite, 1984; Spite & Spite, 1986; Rebolo, Molaro & Beckman, 1988, hereafter RMB; but see also Thorburn, 1994).

The substantial flatness of the plateau and the absence of intrinsic scatter (Spite et al., 1996; Bonifacio & Molaro, 1997), coupled with the detection of the fragile isotope ${}^6\text{Li}$ in the metal-poor stars HD 84937 (Smith et al., 1993; Hobbs & Thorburn, 1997; Cayrel et al., 1999) and perhaps BD+42 2667 (Cayrel et al., 1999), are the arguments for claiming that no significant depletion mechanisms should have acted in these stars to modify the pristine ${}^7\text{Li}$ abundance (but see also Ryan, Norris & Beers, 1999).

We also note a competing theory, which claims that the highest ${}^7\text{Li}$ abundance - measured in the most Li-rich Population I objects - is the primordial one (Boesgaard et al., 1998). In this case some depletion mechanisms able to deplete Li in all the halo stars by the same amount acting on a Galactic lifetime timescale are required. Possible mechanisms include diffusion (Vauclair, 1988), rotational mixing (Pinsonneault et al., 1992) and stellar winds (Vauclair and Charbonnel, 1995).

Recently, Fields & Olive (1998), using a standard model of Galactic cosmic ray (GCR) nucleosynthesis, found that only little ${}^6\text{Li}$ (and ${}^7\text{Li}$) depletion is allowed in halo stars. So that the observed Spite plateau should be indicative of the primordial Li abundance.

Younger stars span a wide range of lithium abundances. The highest values, measured in Orion T Tauri

stars reach $A(\text{Li})^1 \sim 3.83$ dex (~ 3.5 dex when corrected for NLTE effects, Duncan & Rebull, 1996). Therefore, some mechanisms of ${}^7\text{Li}$ production are required to increase the Li abundance from the plateau value to the present one. Nuclear reactions in stellar interiors and spallation processes on interstellar medium (ISM) particles involving either high or low energy GCRs have both been proposed as possible mechanisms able to synthesize ${}^7\text{Li}$ and restore it back to the ISM, where it enters into the chemical composition of the new-formed stars.

Lithium evolution has already been studied in detail by several authors. D’Antona & Matteucci (1991), by means of a complete model of chemical evolution, have shown that both the Solar System lithium abundance and the rise from the Spite plateau could be explained assuming Li-production in classical novae and AGB stars. Later, novae were ruled out as lithium producers at a Galactic level (Boffin et al., 1993). Matteucci et al. (1995) suggested a combination of ν -process nucleosynthesis from Type II SNe and hot bottom burning in intermediate mass AGB stars to match the observations. Recently, Matteucci et al. (1999) used the same nucleosynthesis prescriptions to calculate the expected ${}^7\text{Li}$ content in the Galactic bulge. Lithium production by low mass AGB stars (C-stars) and standard GCR nucleosynthesis were the key ingredients of the model of Abia et al. (1995), which was able to match also the behaviour of the lithium isotopic ratio. In any case, they had to require a percentage of Li-rich C-stars much higher (6–8%) than observed (2–3%). However, we note that C-stars at low metallicities are found much more numerous ($\sim 10\%$, Beers et al., 1992; Norris et al., 1997).

In this paper we deal with Galactic lithium evolution taking into account the lithium production both in stars and from GCRs. The aim of the paper is to reproduce the observed upper envelope of the diagram $A(\text{Li})$ vs $[\text{Fe}/\text{H}]$, assuming that the Population II ${}^7\text{Li}$ is the primordial one. In §2 we present the data-set we have used to constrain the model results, in §3 we review the main candidates as stellar lithium producers, in §4 we present the basic assumptions of the chemical evolution model and the lithium synthesis prescriptions, in §5 we illustrate our main results and in §6 we draw some conclusions.

2. Observational data

The observed evolution of the ${}^7\text{Li}$ abundance with metallicity, when abundance determinations in disk and halo dwarfs are restricted to stars with effective temperature $T_{\text{eff}} \geq 5700$ K, suggests that there is a general trend towards a larger ISM ${}^7\text{Li}$ content with increasing metallic-

ity. In previous papers (e.g. Matteucci et al., 1995, 1999) the abundances used to constrain Galactic chemical evolution models were pointing to a smooth increase from the Spite plateau to the Solar System value. In this paper we show the results of an analysis performed on a large selection of data taken from the literature. Li detections for those stars which are tracing the upper envelope of the observational $A(\text{Li})$ vs $[\text{Fe}/\text{H}]$ diagram have been critically analysed and a rise off the plateau steeper than previously assumed has been found. This result, coupled with a Spite plateau which extends towards larger metallicities, suggests a revision of the various contributions to the ${}^7\text{Li}$ production from different sources. In particular, ${}^7\text{Li}$ producers restoring their lithium to the ISM on long timescales should be preferred.

${}^7\text{Li}$ measurements in stellar atmospheres have been selected from the literature in the metallicity range $-1.5 \leq [\text{Fe}/\text{H}] \leq -0.5$ dex². This region is particularly interesting because it is the metallicity range where the observed lithium abundance is expected to start growing due to ${}^7\text{Li}$ injection from the first Li factories.

From the point of view of stellar nucleosynthesis, it is important to determine the metallicity at which the Li abundance starts rising off the Spite plateau. For instance, the constancy of the Spite plateau at $[\text{Fe}/\text{H}] \leq -1.5$ translates into the requirement that Type II SNe coming from the first stellar generations should contribute only an amount of lithium smaller than the primordial one.

Selection criteria have been applied in order to remove from the sample all those stars which are likely to have passed through phases during which they either destroyed or diluted their initial lithium content. To this purpose, we selected only stars not suffering any ${}^7\text{Li}$ convective depletion, i.e. $T_{\text{eff}} \geq 5700$ K, according to standard models. Stars with $T_{\text{eff}} < 5700$ K are cool enough to be threatened by Li burning in deep convective envelopes already during the pre-main sequence (see also Ryan & Deliyannis, 1998). Moreover, we retained only stars included in the HIPPARCOS catalogue which provides accurate information on kinematics and luminosities. Objects recognized as giants or subgiants are likely to show Li surface abundances affected by dilution and have been rejected.

The program stars are listed in Tab.3. For each star we give the HD, DM, G and HIP numbers and the U, V, W heliocentric space-velocity components with the associated errors. The membership to a specific Galactic popula-

¹ $A(\text{Li}) = \log_{10} (N_{7\text{Li}}/N_{\text{H}}) + 12$.

² Sources in the literature: Deliyannis et al., 1990; Lambert et al., 1991; Pilachowski et al., 1993; Pasquini et al., 1994; Spite et al., 1996.

tion (halo or disk, either thin or thick) as derived from the kinematics and the evolutionary status are also provided.

2.1. Evolutionary status

In order to determine the evolutionary status of each star in our sample, we used the theoretical isochrones by Bertelli et al. (1994). We divided the program stars in three metallicity bins ($[\text{Fe}/\text{H}] \geq -0.75$; $-1.25 \leq [\text{Fe}/\text{H}] \leq -0.75$; and $[\text{Fe}/\text{H}] \leq -1.25$). For each bin the data were compared with theoretical isochrones appropriately chosen for different ages at different metallicities. In the bin $[\text{Fe}/\text{H}] \geq -0.75$ we used the isochrones of 2–9 Gyr; in the bin $-1.25 \leq [\text{Fe}/\text{H}] \leq -0.75$ the 6–19 Gyr isochrones, and in the bin $[\text{Fe}/\text{H}] \leq -1.25$ those of 8–20 Gyr. The absolute magnitudes for the stars in our data-base were obtained from the HIPPARCOS parallaxes. The effective temperatures were calculated using the $(B - V) - T_{\text{eff}}$ calibration of Alonso et al. (1996). Within each metallicity bin and by using the appropriate isochrone we distinguished among turn-off, giant and subgiant stars following the criteria outlined by Beers et al. (1990). We found that most of the stars are turn-off stars; only few among them (HIP 36430, HIP 37723, HIP 86694, HIP 103987, HIP 115167, HIP 116082) are subgiants and are, therefore, not considered in the analysis.

2.2. Kinematics

The heliocentric Galactic space-velocity components, U , V and W , calculated from the star’s proper motion, parallax and radial velocity following the Johnson & Soderblom (1987) analysis, are listed in columns 5, 6, 7 of Tab.3. The uncertainties σ_U , σ_V and σ_W are also given in columns 8, 9, 10. A left-handed coordinate system for U , V , W , so that they are positive in the directions of the Galactic anticenter, the Galactic rotation and the North Galactic Pole, respectively, is adopted. The radial velocities used to complement HIPPARCOS data are from the SIMBAD data-base or from the literature. For 12 objects lacking of radial velocity U , V , W are not provided. Stars for which the relative error on the parallax is greater or equal to 100% ($\sigma_\pi/\pi \geq 1$) have also no kinematics determination.

With these data at hand we distinguished between a *disk population* and a *non-disk population*. Adopting a selection criterium based on the studies by Sandage & Fouts (1987) and Beers & Sommer-Larsen (1995), in order to belong to the disk population we required a star to have $V > -115 \text{ Km s}^{-1}$ and $(U^2 + W^2)^{\frac{1}{2}} < 150 \text{ Km s}^{-1}$.

In Fig.1 we show the V vs $(U^2 + W^2)^{\frac{1}{2}}$ diagram obtained for our data sample. Stars with metallicities below or above $[\text{Fe}/\text{H}] = -1.0$ are shown with different symbols.

In this plot the kinetic energy associated to the rotation around the Galactic center is compared to the kinetic energy associated to any other motion. As expected, stars with $[\text{Fe}/\text{H}] > -1.0$ concentrate in the region $V > -50 \text{ Km s}^{-1}$, $(U^2 + W^2)^{\frac{1}{2}} < 100 \text{ Km s}^{-1}$ and dilute outside. These objects compose the bulk of the Galactic *disk*. The *thick-disk* should be envisaged in those stars which rotate more slowly and with larger random motions. For the sake of simplicity, we choose here to distinguish only between disk and non-disk stars.

Contrary to common assumption that all halo stars are also metal-poor we found three stars G 170-156 ($[\text{Fe}/\text{H}] = -0.8$, HIP 86321), G 17-21 ($[\text{Fe}/\text{H}] = -0.6$, HIP 80837) and G 182-19 ($[\text{Fe}/\text{H}] = -0.7$, HIP 86431) with metallicities larger than $[\text{Fe}/\text{H}] > -1.0$ which do not show disk-like motion. One more star BD+01 3421 ($[\text{Fe}/\text{H}] = -0.5$, HIP 84905) is possibly belonging to the thick-disk.

On the other hand we found three stars HD 166913 ($[\text{Fe}/\text{H}] = -1.8$, HIP 89554), HD 205650 ($[\text{Fe}/\text{H}] = -1.3$, HIP 106749) and HD 134169 ($[\text{Fe}/\text{H}] = -1.6$, HIP 74079) with metallicity below -1.0 which possess a disk-like motion. These three stars are members of the metal-weak tail of the Galactic disk. Other two stars with these properties have been found by Bonifacio et al. (1999).

Five stars (HIP 104659, HIP 37789, HIP 11952, HIP 37853 and HIP 55022) are lying just on the boundary which separates the halo from the disk stars.

In order to ascertain a possible correlation between the kinematics of the stars and the ${}^7\text{Li}$ abundance, we drew in Fig.2 the graph $A(\text{Li}) - [\text{Fe}/\text{H}]$ indicating with different symbols disk stars, non-disk stars and objects without a precise kinematical membership. From Fig.2 we note that the star HD 160693 (HIP 86431), with halo-like motion and a metallicity of -0.7 , has $A(\text{Li}) < 1.2$ falling well below the Li plateau. On the other hand the metal-poor stars with disk motions show a Li abundance at the plateau level. Thus lithium depletion is likely related only to metallicity and independent from the kinematics.

These findings allow us to assume that the upper envelope of the observational diagram traces those stars which have suffered only a minor lithium depletion during their life. This interpretation is also supported by the analysis of the stars with Be data, whose Be abundances imply Li abundances larger than actually observed (Molaro et al., 1997). Therefore, the upper envelope results from the various lithium enrichment processes occurred during the overall Galactic lifetime.

Our revised compilation of the data from the literature shows a plateau which may extend at metallicities larger than previously assumed and points to a very steep rise off the plateau starting at $[\text{Fe}/\text{H}] \sim -0.5, -0.3$. Details

of the star by star critical Li analysis are provided in appendix.

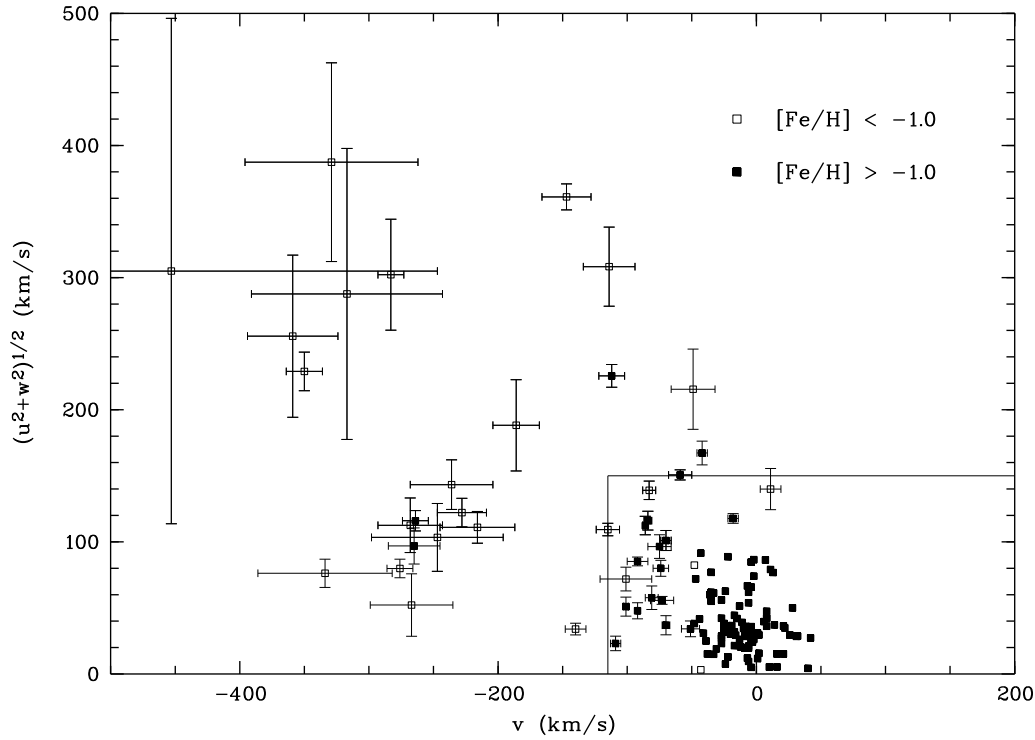


Fig. 1. V versus $(U^2 + W^2)^{\frac{1}{2}}$ diagram for the sample stars. The stars have been divided into two metallicity bins, on the grounds of the metallicity values given in Tab.4. In the case of multiple metallicity determinations we have adopted the average value. $V > -115 \text{ Km s}^{-1}$ and $(U^2 + W^2)^{\frac{1}{2}} < 150 \text{ Km s}^{-1}$ are the two selection criteria which have to be satisfied in order to ascribe the star to the Galactic disk (either thin or thick). For the sake of clarity, no error bars are drawn in the most dense region of the plot. In any case, stars lying in that region have quite small errors associated to the determinations of their velocity components. The stars HIP 106749 (the empty square in the upper left corner of the box) and HIP 74079 (the empty square in the lower left corner of the box) have been offset by $+20 \text{ Km s}^{-1}$ in $(U^2 + W^2)^{\frac{1}{2}}$ and by -40 Km s^{-1} in V , respectively, to make them clearly visible.

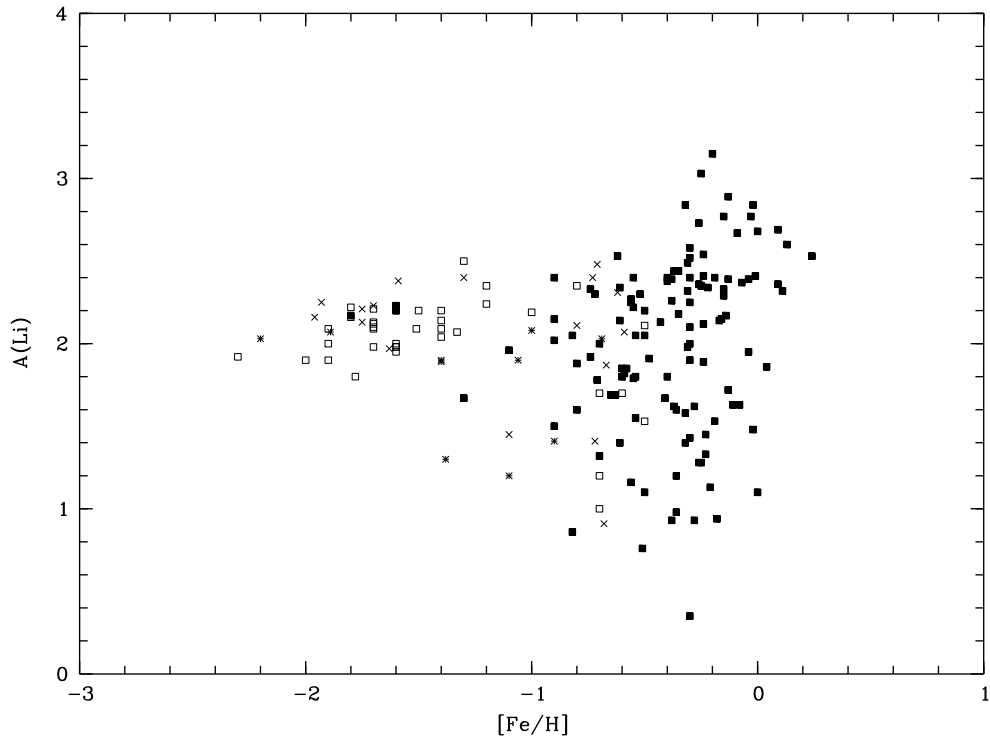


Fig. 2. The observational $A(\text{Li})$ vs $[\text{Fe}/\text{H}]$ diagram. Filled squares: disk stars; empty squares: non-disk stars; asterisks: objects with V_{rad} determination for which we were not able to provide an estimate on the kinematical membership; crosses: objects with no V_{rad} determination. All the entries of Tab.4 have been plotted.

3. Stellar sites for ${}^7\text{Li}$ production

3.1. *Novae as lithium factories*

Both theoretical and observational evidence suggests that classical novae may be responsible for a non-negligible contribution to the ISM pollution in several nuclides (${}^7\text{Li}$, ${}^{13}\text{C}$, ${}^{15}\text{N}$, ${}^{17}\text{O}$) and radioactive isotopes (${}^{22}\text{Na}$, ${}^{26}\text{Al}$) (see Gehrz et al., 1998 for a review on this subject). The nova explosion results from thermonuclear runaway on the surface of a CO or ONeMg white dwarf (WD) accreting hydrogen-rich matter from a main sequence companion which fills its Roche lobe in a close binary system; so the material ejected into the ISM shows a composition enriched in elements synthesized by explosive hydrogen-burning.

The pre-explosion ${}^3\text{He}$ concentration in the accreted envelope plays a key role in determining how much ${}^7\text{Li}$ will be produced in the outburst. Starrfield et al. (1978) found that the ${}^7\text{Li}$ yield does scale linearly with the initial ${}^3\text{He}$ content. Their result was used by D’Antona & Matteucci (1991) who successfully reproduced the upper envelope of the observed $A(\text{Li})$ vs $[\text{Fe}/\text{H}]$ diagram for the solar neighborhood. These authors adopted $A(\text{Li}) = 2.10$ dex as the primordial lithium abundance and explained the observed increasing trend in lithium abundance with time as due to Galactic enrichment coming from lithium production by stellar sources, identified in both novae and AGB stars.

Later, novae nucleosynthesis was discussed by Boffin et al. (1993), who reinvestigated ${}^7\text{Li}$ production in explosive hydrogen-burning with the inclusion of the ${}^8\text{B}(p,\gamma){}^9\text{C}$ reaction and ruled out novae as lithium producers at a Galactic level. In particular, they ruled out the linear dependence of Li production on the ${}^3\text{He}$ abundance in the exploding envelope, which was a key ingredient in the D’Antona & Matteucci model. Boffin et al. used a parameterized one-zone explosive nucleosynthesis model and detailed numerical network calculations to demonstrate how the high peak densities prevailing at the base of the hydrogen-burning shell during the nova outburst prevent the build-up of ${}^7\text{Li}$ amounts sufficient for ISM enrichment. However, they also stressed the need for testing their results by detailed hydrodynamic nova models.

This check was effectively carried out a few years later: Hernanz et al. (1996), using a hydrodynamic code able to treat both the accretion and the explosion stages, have obtained large overproduction factors relative to the solar abundance for ${}^7\text{Be}$ - and hence ${}^7\text{Li}$. Therefore, although the final masses injected in the ISM are small, significant production of ${}^7\text{Li}$ by novae seems possible. In their models, these authors have assumed a solar composition of the infalling material and the existence of processes able to mix

it with the inner layers of the underlying white dwarf. This assumption allows one to obtain the enhanced CNO or ONeMg abundances required in order to give rise to a nova outburst and to explain some observations (see Livio, 1994 for a recent review).

More recently, José & Hernanz (1998) computed an enlarged grid of hydrodynamical nova models for both CO and ONeMg WDs, spanning a total range of white dwarf masses of $0.8 - 1.35 M_{\odot}$. In these models different mixing levels - ranging from 25 to 75% - between the accreted envelope and the underlying WD core were assumed. These models predict ejected quantities of ${}^7\text{Li}$ able to affect the evolutionary history of this nuclide on a Galactic scale.

At this point, it is worth emphasizing the strong dependence of these results on the chemical composition at the onset of the explosion: the predicted ${}^7\text{Li}$ overproduction factors will be correct only if the evolution of ${}^3\text{He}$ during the accretion phase has been followed in the right manner. Moreover, we note that if the underlying WD is a CO one, the predicted ${}^7\text{Li}$ abundances are ~ 1 order of magnitude larger than in the case of an underlying ONeMg WD (see e.g. Table 1 of Hernanz et al., 1996).

3.2. *Lithium production in massive AGB stars*

${}^7\text{Li}$ production in AGB stars is the only Li stellar production mechanism supported by observations.

Smith & Lambert (1990) analysed high-resolution spectra for 27 red giants in the Magellanic Clouds, spanning a range in bolometric absolute magnitudes $M_{bol} \sim -5$ to -9 . They found that Li-rich stars were confined to those with $M_{bol} \sim -6$ to -7 , while lower ($M_{bol} \sim -5$ to -5.5) and higher ($M_{bol} \sim -7$ to -9) luminosity red giants showed no Li features. In addition, all their Li-strong stars presented $\text{C}/\text{O} < 1$ and bore evidence of strengthened s-process atomic lines. These facts were interpreted as a signature of the dredge-up and subsequent envelope burning mechanism, occurring in the massive AGB stars ($M \sim 4 - 8 M_{\odot}$). Since every luminous AGB star observed showed the Li I doublet, it seemed to be very likely that the ${}^7\text{Li}$ produced in the outer envelope was not destroyed quickly, but it was surviving in the stellar atmosphere and injected into the ISM by stellar winds. Smith & Lambert derived a maximum abundance of ${}^7\text{Li}$ as large as $A(\text{Li}) \sim 4.0$ for the luminous AGB stars and indicated them as a major source of ${}^7\text{Li}$ in a galaxy.

These observational findings were confirmed by theoretical calculations in which a time-dependent “convective diffusion” algorithm for the hot bottom envelopes of AGB stars was coupled with a fully self-consistent evolutionary sequence (Sackmann & Boothroyd, 1992). It was shown

that values of $A(\text{Li})$ lying between 4 and 4.5 could be obtained for stars in the luminosity range $M_{bol} \sim -6$ to -7 , in excellent agreement with observations of the most lithium-rich giants in external galaxies (Smith & Lambert, 1990; Smith et al., 1995) but in poorer agreement with observations in our Galaxy (Abia et al., 1991). According to Sackmann & Boothroyd, super-rich lithium giants would occur in the mass range $M \sim 4-6 M_{\odot}$, when the temperature at the base of the convective envelope exceeds 50×10^6 K and the Cameron-Fowler mechanism³ works (in these models, stars with $M \geq 7 M_{\odot}$ ignite carbon in the center before they become AGB stars and never experience hot bottom burning).

Later, Plez et al. (1993) enlarged the Smith & Lambert's sample of giants in the Small Magellanic Cloud (SMC) and pointed out that several of these metal-poor giants have atmospheric abundances of ${}^7\text{Li}$ too low to provide a significant contribution to Galactic enrichment. On the other hand, Sackmann & Boothroyd had shown that a decrease in the metallicity causes the hot bottom burning to start at smaller masses, resulting in a larger ${}^7\text{Li}$ production! This seems to lead to a discrepancy with Plez et al.'s observations, but it should be recalled that low metallicity giants lose their envelope mass at a smaller rate than more metal-rich giants, thus allowing Li-burning to occur before the planetary nebula (PN) ejection and thus preventing significant ISM pollution and explaining Plez et al.'s findings.

Recent studies (Mazzitelli et al., 1999) confirm that ${}^7\text{Li}$ abundances as large as $A(\text{Li}) \sim 4.0$ dex at maximum can be found in the atmospheres of massive AGB stars.

The ${}^7\text{Li}$ production by C-stars (coming from progenitors in the mass range $2-5 M_{\odot}$) can be regarded as negligible on a Galactic scale, on the ground of the very small number of Li-rich C-stars detected with respect to their total number (see Wallerstein & Conti, 1969; Abia et al., 1993a, 1993b; but see also Beers et al., 1992). Such a low number of Li-rich C-stars can be easily explained if it is assumed that these stars represent a short-lived phase with respect to the overall stellar lifetime on the AGB. On the contrary, one should assume that for stars with progenitor masses in the range $5-8 M_{\odot}$ the envelope ejection in the PN stage shortly follows the lithium production in the envelope itself. We want to recall briefly that lithium production in these stars is thought to be due either to hot bottom burning, occurring during thermal pulses (TPs) at the base of the common envelope, or to a mechanism such as that described by Iben (1973), involving only the region

of the outer convective envelope lying near the hydrogen burning shell, during the long timescale of the interpulse phases.

3.3. ${}^7\text{Li}$ synthesis in Type II supernova explosions

${}^7\text{Li}$ synthesis in massive stars ($M > 10 M_{\odot}$) is theoretically explained as being due to a particular mechanism, the neutrino process. The first realistic exploration of the so-called neutrino process (ν -process), acting during SNeII explosion, was undertaken by Woosley et al. (1990). Such a process occurs in the shells overlying the collapsing core of a contracting massive star. In these conditions, the flux of neutrinos is so large that, despite the small cross section, evaporation of neutrons or protons from heavy elements and helium is expected. The back reaction of these nucleons on other species alters the outcome of traditional nucleosynthesis calculations, resulting in a large production of a great number of rare isotopes. ${}^7\text{Li}$ is one of these; it is thought to be made mainly in the helium and in the silicon shells from μ - and τ -neutrinos interacting with helium. In their work, Woosley et al. strongly supported the idea that this lithium production by ν -process in massive stars could be large enough to explain the full ${}^7\text{Li}$ Solar System abundance.

This point was later revised when Timmes et al. (1995), using the output from a grid of 60 Type II supernova models of varying mass and metallicity (Woosley & Weaver, 1995), computed the chemical evolution of several stable isotopes, taking into account also the nucleosynthesis from Type Ia supernovae and from single stars with $M \leq 8 M_{\odot}$. They found that massive stars are producing lithium prior to $[\text{Fe}/\text{H}] \sim -1.0$ dex, but until this metallicity value the contributions are small compared to the infall values, thus preserving the flat shape of the diagram $A(\text{Li})$ vs $[\text{Fe}/\text{H}]$ inferred from the observations. Finally, they concluded that Type II supernovae contribute about one-half the solar ${}^7\text{Li}$ abundance⁴, pointing to a lower ${}^7\text{Li}$ production rate by the ν -mechanism than Woosley et al. (1990). Such an outcome was confirmed also by Matteucci et al.'s (1995) analysis, where C-stars plus massive AGB stars on the one hand and Type II SNe on the other hand were found to contribute each one-half the Solar System ${}^7\text{Li}$ abundance, although the authors did not conclusively rule out a fraction between 1/4 and 3/4 from both sources, because of the uncertainties in the input nucleosynthesis.

³ See Cameron & Fowler (1971) for a detailed description of this mechanism.

⁴ This result is achieved for μ - and τ -neutrino temperatures in the range 6–8 MeV, which is the range suggested by SN 1987 A.

4. The model

4.1. Basic assumptions

The adopted model of chemical evolution is that of Chiappini et al. (1997), in which we included the ${}^7\text{Li}$ evolution, taking into account Li production from all the stellar sources identified above and from GCR spallation. This model assumes that the halo and thick-disk formed quickly (on a timescale of ~ 2 Gyr) during a first infall episode and the thin-disk formed on a much larger timescale (~ 8 Gyr) during a second independent infall episode.

The nova system nucleosynthesis has been included in the model in a detailed way under simple hypotheses. We first computed the nova systems formation rate at the time t as a fraction of the formation rate of white dwarfs at a previous time $t - \Delta t$ as in D’Antona & Matteucci (1991):

$$R_{novae}(t) = \alpha \int_{0.8}^8 \psi(t - \tau_m - \Delta t) \phi(m) dm.$$

Here Δt is a delay time whose value has to be fixed to guarantee the cooling of the WD at a level that ensures a strong enough nova outburst. We chose $\Delta t = 1$ Gyr as a suitable average value (D’Antona, 1998) and assumed that all stars with initial masses in the range $0.8 - 8 M_{\odot}$ end their lives as WDs.

$\psi(t)$ is the star formation rate (SFR), τ_m is the lifetime of the star of mass m and $\phi(m)$ is the initial mass function (IMF). More about SFR and IMF parameterization can be found in Chiappini et al. (1997) concerning the disk of the Galaxy and in Matteucci et al. (1999) concerning the Galactic bulge.

The rate of nova eruptions is related to the WD formation rate:

$$R_{outbursts} = \alpha R_{WDs} n,$$

where αR_{WDs} is the formation rate of WDs in binary systems which will give rise to nova eruptions, and $n = 10^4$ is the average number of nova outbursts for a typical nova system (Bath & Shaviv, 1978; see also Shara et al., 1986). The parameter α , set equal to a constant value along the overall evolutionary history of the Galaxy, can be fixed by the rate of nova outbursts in our galaxy at the present time. Estimates of this quantity in the current literature range from as few as 11 to as many as 260 nova outbursts yr^{-1} . In particular, predictions based on scalings from extragalactic nova surveys suggest low values ($11 - 46 \text{ yr}^{-1}$, Ciardullo et al., 1990; $15 - 50 \text{ yr}^{-1}$ - with the lowest values, between 15 and 25 yr^{-1} , strongly favored - Della Valle & Livio, 1994), whereas estimates based on extrapolations of Galactic nova observations give the highest rates ($73 \pm$

24 yr^{-1} , Liller & Mayer, 1987; 260 yr^{-1} , Sharov, 1972; 50 yr^{-1} , Kopylov, 1955; 100 yr^{-1} , Allen, 1954)⁵. We chose for the present time rate of nova outbursts in the Galaxy $R_{outbursts}(t_{Gal}) \sim 25 \text{ yr}^{-1}$ for the following reasons: (1) observation of novae in nearby galaxies would avoid, or at least minimize, most of the problems encountered by Galactic observations; (2) a recent study of Shafter (1997) shows that the nova rate based on Galactic observations can be made consistent with the rate predicted from the extragalactic data, particularly if the Galaxy has a strong bar oriented in the direction of the Sun (in this latter, most favourable case, the suggested value is near $\sim 20 \text{ yr}^{-1}$, otherwise, if the bar is weak or misaligned, the global rate can be reduced only to $\sim 30 \text{ yr}^{-1}$).

4.2. Nucleosynthesis prescriptions

We assumed a homogeneous Big Bang ${}^7\text{Li}$ abundance of 2.2 dex (Bonifacio & Molaro, 1997) as the primordial one and considered all the contributions from the various classes of stellar ${}^7\text{Li}$ factories seen in §3 in the Galactic chemical evolution model.

In this study we adopted the updated lithium yields from theoretical nova outbursts provided by José & Hernanz (1998). We took the mean mass ejected as ${}^7\text{Li}$ averaged on 7 evolutionary sequences for CO WDs and the mean mass ejected as ${}^7\text{Li}$ averaged on so many evolutionary sequences for ONeMg WDs. ONeMg WDs are believed to originate from stars with initial masses in the range $7 M_{\odot} - M_{up}$ ⁶ (but there is still debate on this point). Since the lifetime of a $7 M_{\odot}$ star is ~ 0.045 Gyr, we assumed that for $t \leq 0.045$ Gyr only ONeMg WDs can contribute to nova systems; for times larger than 0.045 Gyr, about 30% of novae occur in systems containing ONeMg WDs, while the remaining take place in systems accreting hydrogen-rich envelopes onto CO WDs.

In particular, the prescriptions for ${}^7\text{Li}$ yields from novae we used in our model are as follows:

for $t < 0.045$ Gyr we assumed

$$M_{ej} = 1.95 \times 10^{-1} M_{\odot}$$

(mean mass ejected by a single nova system during its overall evolution) and

$$X_{7Li} = 9.24 \times 10^{-7}$$

⁵ Hatano et al. 1997 reanalyzed Liller & Mayer’s data and argued that the correct rate should be $\sim 41 \text{ yr}^{-1}$ rather than $73 \pm 24 \text{ yr}^{-1}$.

⁶ Here we assume M_{up} , the limiting mass for the formation of a degenerate CO core, equal to $8 M_{\odot}$, although some authors suggest $5 - 6 M_{\odot}$ as a more suitable value, when overshooting is taken into account (Chiosi et al., 1992; Marigo et al., 1996).

(mean ${}^7\text{Li}$ abundance - in mass fraction - in the ejected material).

For $t > 0.045$ Gyr we assumed

$$M_{ej} = 2.63 \times 10^{-1} M_{\odot}$$

with

$$X_{7\text{Li}} = 2.85 \times 10^{-6}$$

as the mean lithium abundance in the ejected envelope.

As far as AGB stars are concerned, we included here a metallicity dependence of the lithium yields from massive AGB stars as in Matteucci et al. (1995), which accounts for the lower ${}^7\text{Li}$ abundances observed in the low metallicity SMC AGB stars relative to the higher ones exhibited by their more metal-rich Galactic counterparts. We assumed no production of lithium by AGB stars until a metallicity of $Z = 10^{-3}$, then allowing lithium production only in the mass range $5 M_{\odot} - M_{up}$, where M_{up} increases from 5 to $8 M_{\odot}$ as Z reaches the solar value. The ${}^7\text{Li}$ abundance in the ejected material is assumed to be either $A(\text{Li}) = 4.15$ or $A(\text{Li}) = 3.50$ dex (see Tab.1 for different model prescriptions). Since only a small number of Li-rich C-stars (coming from progenitors with masses in the range $2 - 5 M_{\odot}$) are known out of hundreds of C-stars observed in the Galaxy and in the Magellanic Clouds, we assumed their contribution to the lithium enrichment to be almost negligible and followed the D'Antona & Matteucci (1991) prescriptions. In one model (model C) we also completely suppressed this class of lithium factory.

To account for lithium production in Type II supernovae, we considered the metallicity dependent ${}^7\text{Li}$ yields given by Woosley & Weaver (1995). We included in our computation both the full yields (model A and B) and those reduced to a half (model C).

${}^7\text{Li}$ astration in stars of all masses has also been taken into account.

The contribution of GCR spallation has been taken into account by incorporating the absolute yields from Lemoine et al. (1998) into the chemical evolution model. We took the yields from the lower-bound spectrum in their Table 1.

Table 1. Nucleosynthesis prescriptions.

Model	C-stars	M-AGB	SNeII	novae
A	$A(\text{Li}) = 3.85$	$A(\text{Li}) = 4.15$	WW95	no
B	$A(\text{Li}) = 3.85$	$A(\text{Li}) = 4.15$	WW95	yes
C	no	$A(\text{Li}) = 3.50$	WW95/2	yes

5. Results

In Fig.3 we show the predicted $\log(R_{WDs})$, $\log(R_{novae})$ trends vs time in the solar neighborhood for models with $\alpha = 0.0125$. By assuming a Galactic scale height of 300 pc for WDs - and hence novae - and a Galactic volume of 10^{11} pc^3 we obtain $R_{outbursts}(t_{Gal}) = 24.5 \text{ yr}^{-1}$, in good agreement with observations (see section 4.1).

We predict also that the current WD birthrate in the Galaxy should be $R_{WDs}(t_{Gal}) = 2.27 \times 10^{-12} \text{ WDs pc}^{-3} \text{ yr}^{-1}$, to be compared with observational estimates which give $R_{WDs}(t_{Gal}) = 1 \times 10^{-12} \text{ WDs pc}^{-3} \text{ yr}^{-1}$ (Yuan, 1989) and D_{WDs} (spatial density) $\sim 1 \times 10^{-2} \text{ pc}^{-3}$ (Weidemann, 1967). This slight discrepancy, however, can be explained by recent dynamical calculations (Chamcham, 1998) suggesting that about 40% of the white dwarfs originally formed in the thick-disk have moved from their birthplaces so that they should be observed at a higher scale height at the present time.

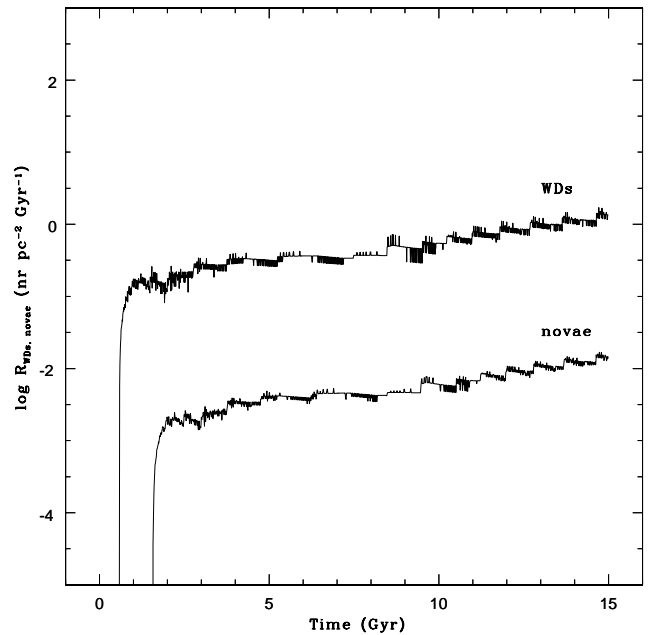


Fig. 3. Birthrates of white dwarfs and nova systems as functions of time, predicted with the two-infall Galactic chemical evolution model that considers a threshold in the surface gas density below which star formation is suppressed (see text for details). The nova systems formation rate is assumed to be a fraction $\alpha = 0.0125$ of the WDs formation rate.

Note that the oscillations in the theoretical curves in Fig.3 are caused by the introduction of a threshold in the surface gas density ($7 M_{\odot} \text{ pc}^{-2}$) below which star forma-

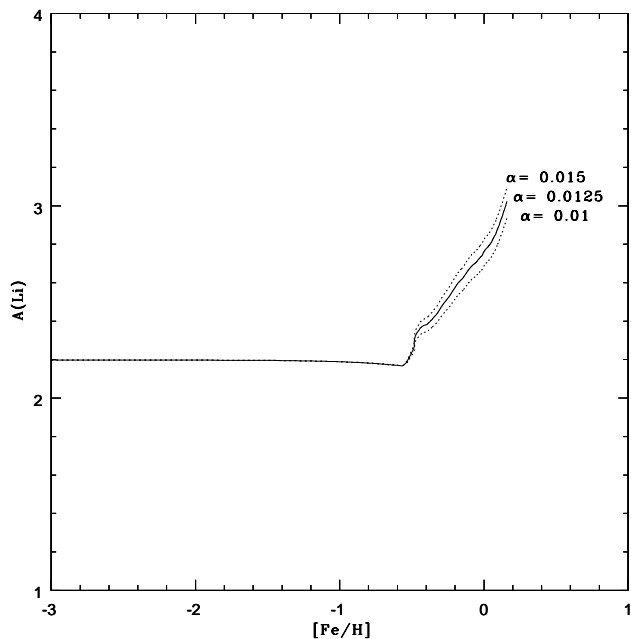


Fig. 4. $A(\text{Li})$ vs $[\text{Fe}/\text{H}]$ theoretical trends predicted for the solar neighborhood by three models taking into account lithium production in nova outbursts under slightly different assumptions on the percentage of newly formed WDs that enters in the building-up of nova systems.

tion stops, owing to gas instability against density condensations in these conditions (see Chiappini et al., 1997). The presence of such a threshold leads also to a delay in the WD formation, which starts only after ~ 0.6 Gyr (compare Fig.3 here with Fig.2 in D’Antona & Matteucci, 1991, whose model does not include such a threshold in the gas density).

We ran several models considering separately all the ${}^7\text{Li}$ stellar sources discussed above. The Galactic lithium enrichment in the solar neighborhood due only to novae is sketched in Fig.4: novae start injecting material into the ISM with a time delay of ~ 2 Gyr, when the ISM has already achieved a metallicity $[\text{Fe}/\text{H}] \sim -0.5$ dex. This long time-lag in the occurrence of an ISM pollution by novae is the direct consequence of two elements characterizing the evolution of such systems, both acting in the same direction: 1) the time-lag required to form the WD and 2) the time necessary for the WD to cool enough to allow strong nova outbursts.

The effects produced by changing α from 0.0125 to smaller or greater values on the predicted $A(\text{Li})$ vs $[\text{Fe}/\text{H}]$ trend are also shown in Fig.4. We analysed two possible different choices, $\alpha = 0.01$ and $\alpha = 0.015$. The first choice leads to $R_{\text{outbursts}}(t_{\text{Gal}}) = 19.6 \text{ yr}^{-1}$, the second one to

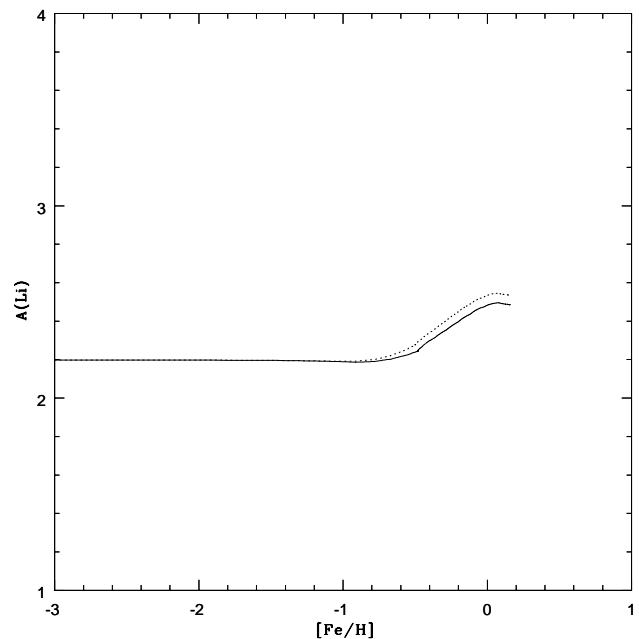


Fig. 5. Accounting for lithium production by both C-stars and massive AGB stars (dotted line) one obtains a slightly higher ${}^7\text{Li}$ abundance at the present time than in the case in which only massive AGB stars are considered (continuous line).

$R_{\text{outbursts}}(t_{\text{Gal}}) = 29.4 \text{ yr}^{-1}$. These estimates reproduce very well the lower and upper limits of the permitted values inferred from the analysis of Shafter (1997). We have chosen $\alpha = 0.0125$ as the most suitable value and used it in all the calculations.

In Fig.5 we show the evolution of the ${}^7\text{Li}$ abundance in the solar neighborhood as predicted by two models both allowing lithium production to happen only in AGB stars (prescriptions on lithium production as in model A). If we assume ${}^7\text{Li}$ production to take place in both C-stars and massive AGB stars (dotted line) we obtain a slightly higher ${}^7\text{Li}$ abundance than assuming ${}^7\text{Li}$ production only in massive AGB stars (continuous line).

In Fig.6 we show the effect of ${}^7\text{Li}$ production only by massive stars. We used either the full ${}^7\text{Li} + {}^7\text{Be}$ yields (Woosley & Weaver, 1995) or the same yields reduced to one half.

From figures 4, 5 and 6 we can immediately see how novae, giving rise to a strong Li-enrichment at high metallicities, can in principle account for the present ${}^7\text{Li}$ abundance in the gas without any other stellar source. However, acting on evolutionary timescales as long as 1.5 Gyr at least, they cannot justify at the same time the rise off the Spite plateau. On the other hand, Type II supernovae start restoring their ${}^7\text{Li}$ into the ISM at earlier times, but

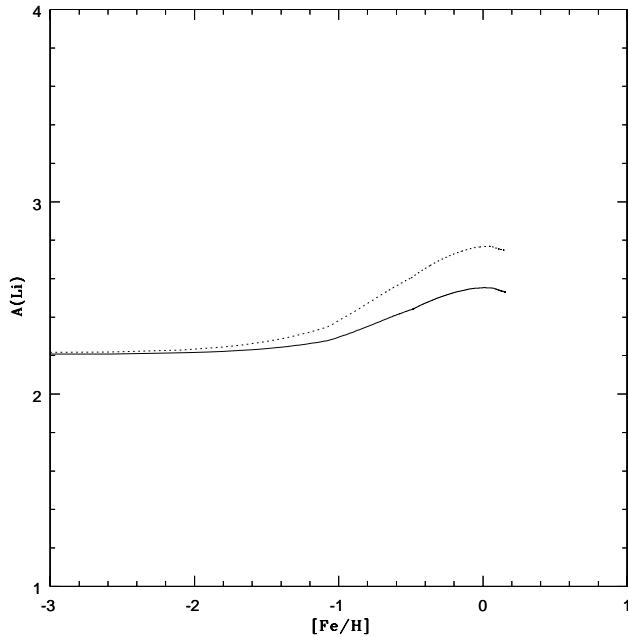


Fig. 6. Theoretical predictions for the trend $A(\text{Li})$ vs $[\text{Fe}/\text{H}]$ from two models when only ${}^7\text{Li}$ production from massive ($M > 10 M_{\odot}$) stars is allowed. Dotted line: we used the Woosley & Weaver (1995) ${}^7\text{Li} + {}^7\text{Be}$ yields; continuous line: we used the same yields but reduced to a half. Note that the metallicity dependence of such yields guarantees the flatness of the Spite plateau until $[\text{Fe}/\text{H}] \sim -1.0$.

they are not able to fully explain the present gas content of lithium, if they are not coupled to other stellar Li producers. The AGB stars present a quite similar behaviour, but restore their ${}^7\text{Li}$ a bit later than SNeII, and in minor (if not almost equal) amounts (compare Figs.5 and 6). Therefore, one single stellar category of ${}^7\text{Li}$ producers could never explain all the observed features of the diagram $A(\text{Li})$ vs $[\text{Fe}/\text{H}]$, under realistic prescriptions about ${}^7\text{Li}$ synthesis!

Therefore we computed three different chemical evolution models for both the solar vicinity and the Galactic bulge, adding together the different stellar sources.

In Figs.7 and 8 we sketch the $A(\text{Li})$ vs $[\text{Fe}/\text{H}]$ trends obtained in the case of the solar neighborhood evolution and in the case of the bulge evolution, respectively. Models A, B and C are referring to the different nucleosynthesis prescriptions outlined in Tab.1. The observational points plotted in Fig.7 are those given in Tab.4 after the upper limits have been removed. An average value has been taken for the three objects with multiple ${}^7\text{Li}$ detections which are tracing the upper envelope (see the appendix). From Fig.7, we see that model A, using the

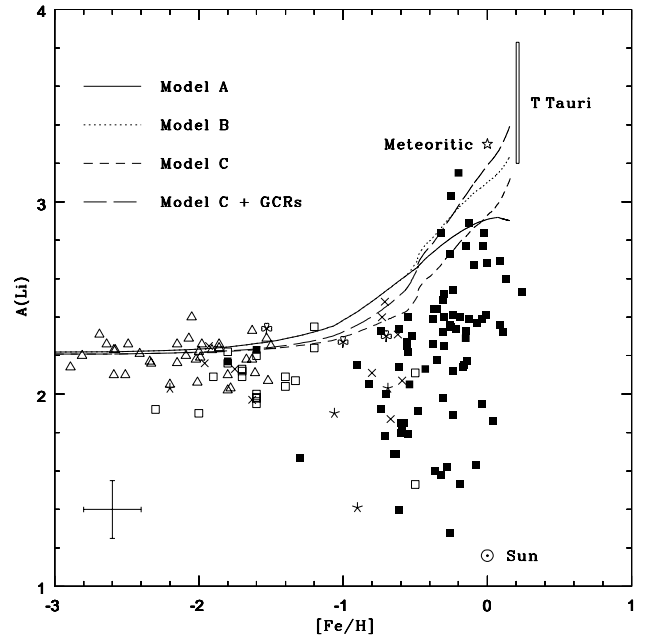


Fig. 7. $A(\text{Li})$ versus $[\text{Fe}/\text{H}]$ theoretical predictions for the solar neighborhood from models A, B, C, and C + GCRs (see text), compared with the observational diagram coming out from our data analysis. The upper limits have been removed from the sample. Filled symbols: disk stars; empty symbols: non-disk stars (triangles: halo stars from Bonifacio & Molaro, 1997; squares: stars from our data-base). Crosses and asterisks identify stars without kinematical membership determination; clovers are objects with multiple ${}^7\text{Li}$ determination in the literature for which we took the average value. Solar, meteoritic (Anders & Grevesse, 1989) and T Tauri (see text for references) ${}^7\text{Li}$ abundances are also shown.

nucleosynthesis prescriptions from the best model of Matteucci et al. (1995), does not reproduce the highest values of $A(\text{Li})$, found in some of the most metal-rich stars, nor the observed upper envelope in the metallicity range $-1.5 \leq [\text{Fe}/\text{H}] \leq -0.5$ dex. Model B, constructed by adding the contribution from nova outbursts to the previous one, produces a curve which becomes much steeper at the highest metallicities, hardly reaching the highest Li abundances exhibited by the most metal-rich stars in our sample. In model C, lithium production from C-stars is set to zero, and ${}^7\text{Li}$ yields from both massive AGB stars and TypeII SNe are reduced. In particular, SNeII yields are assumed to be one half of the original ones. As one can see from Fig.7, model C reproduces at best the observational data in the metallicity range $-1.5 \leq [\text{Fe}/\text{H}] \leq -0.5$, but fails in reproducing the meteoritic and the T Tauri ${}^7\text{Li}$ abundances. ${}^7\text{Li}$ production from GCR spalla-

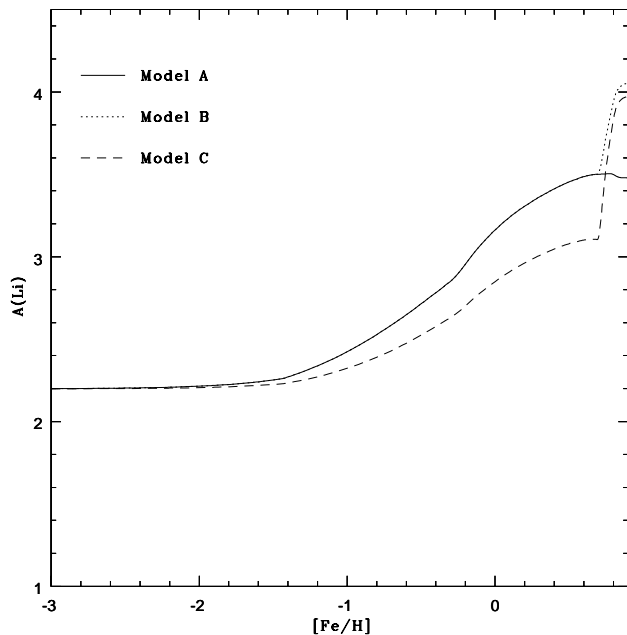


Fig. 8. Theoretical predictions on ${}^7\text{Li}$ abundance evolution in the ISM in the Galactic bulge. Model A (best model in Matteucci et al., 1999), accounting for ${}^7\text{Li}$ production by all stellar sources but novae, predicts the lowest present lithium abundance in the gas in the central region.

tion could be helpful in reproducing the highest observed ${}^7\text{Li}$ abundances.

Molaro et al. (1997), by studying a large sample of stars with ${}^9\text{Be}$ determinations, found that $A(\text{Be})^7$ correlates linearly with $[\text{Fe}/\text{H}]$, with a slope confirmed also by Duncan et al. (1997) and García-López et al. (1998). ${}^9\text{Be}$ is produced only by GCR spallation. Using the Steigman & Walker (1992) formula, ${}^7\text{Li}/{}^9\text{Be} = 7.6$ for PopII stars with $T_{\text{eff}} < 6200$ K, one can see that the ${}^7\text{Li}$ amount expected from GCR spallation alone is about 1% of the primordial ${}^7\text{Li}$ abundance at $[\text{Fe}/\text{H}] \sim -2.5$, and that it becomes more important with increasing metallicity, being about 25% around $[\text{Fe}/\text{H}] \sim -1.0$. At larger metallicities one could expect an even larger contribution, although other authors suggest that GCRs can contribute to the present ISM ${}^7\text{Li}$ abundance by no more than $\sim 10\%$, on the basis of the ${}^7\text{Li}/{}^6\text{Li}$ ratio towards ζ Oph (e.g. Lemoine et al., 1995). In order to include GCR nucleosynthesis in our chemical evolution model in a self-consistent way, we used the absolute yields provided by Lemoine et al. (1998) for various metallicities. As a result, we produced a smoother rise from the plateau, and we were finally able

to match the meteoritic and T Tauri lithium abundances (see Tab.2).

The lithium abundance in the Galactic bulge at the present time predicted by our model C is as high as ~ 4 dex (Fig.8); if novae are not included in the computation, a lower present Li abundance is expected in the bulge (~ 3.5 dex, see also Matteucci et al., 1999). However, this is only a lower limit, since ${}^7\text{Li}$ production from GCRs was not included in the bulge model. In fact, giving the uncertainties in the relevant parameters (see Lemoine et al., 1998), it seems not so meaningful to translate the GCR nucleosynthesis results for the solar neighborhood to the central region of the Galaxy.

Table 2. ${}^7\text{Li}$ abundances at the epoch of Solar System formation and in the interstellar medium as predicted by our four models for the solar neighborhood.

Model	$A(\text{Li})_{\text{SS}}$	$A(\text{Li})_{\text{ISM}}$
A	2.91	2.90
B	3.12	3.24
C	2.95	3.12
C + GCRs	3.21	3.39

6. Conclusions

In this paper we have computed the evolution of the ${}^7\text{Li}$ abundance in the ISM of the solar neighborhood and the bulge of our Galaxy.

We took into account several stellar ${}^7\text{Li}$ factories (novae, massive AGB stars, C-stars and Type II SNe), together with the GCR contribution. In particular, we adopted new nucleosynthesis prescriptions for novae (José & Hernanz, 1998) and the yields of ${}^7\text{Li}$ of Lemoine et al. (1998) as far as GCR nucleosynthesis is concerned.

We compiled a new data sample for ${}^7\text{Li}$ abundances in the solar neighborhood stars identifying the stars belonging to disk and halo Galactic components on the basis of their kinematics. The identification of metal-rich Li depleted halo stars provides evidence that Li depletion depends from metallicity only, thus supporting the use of the upper envelope in the Li data-set as the true indicator of Li Galactic evolution. The selection of the stars which have likely preserved their ${}^7\text{Li}$ content reveals a possible extension of the Li plateau towards higher metallicities, up to $[\text{Fe}/\text{H}] \sim -0.5, -0.3$, with a steeper rise afterwards. Comparing theoretical predictions with the data we derived the following conclusions:

⁷ $A(\text{Be}) = \log_{10}(N_{9\text{Be}}/N_{\text{H}}) + 12$.

- 1– In order to reproduce the upper envelope of the A(Li) vs [Fe/H] diagram we need to take into account several stellar Li sources: AGB stars, Type II SNe and novae. In particular, novae are required to reproduce the steep rise of A(Li) between the formation of the Solar System and the present time, as is evident from the data we sampled. On the other hand, ${}^7\text{Li}$ yields for SNeII should be lowered by at least a factor of two in order to reproduce the extension of the Spite plateau.
- 2– We produced arguments suggesting that GCRs could be responsible for the production of a non-negligible amount of Li at metallicities larger than $[\text{Fe}/\text{H}] \sim -1.0$ dex. In particular, we showed that without any GCR contribution it is impossible to reach the high values observed in meteorites and T Tauri stars: GCRs are responsible for $\sim 45\%$ of the Solar System ${}^7\text{Li}$ (prescriptions on stellar nucleosynthesis as in model C).
- 3– By adopting the nucleosynthesis prescriptions of our model C for the Galactic bulge, we predicted a lower limit for the present time ${}^7\text{Li}$ abundance in this central region of the Galaxy of the order of 4.0 dex, which is 0.5 dex higher than previously estimated in Matteucci et al. (1999) neglecting the novae contribution.

If new ${}^7\text{Li}$ measurements in stars with $[\text{Fe}/\text{H}]$ around -0.5 dex will confirm the extension of the plateau towards such high metallicities, a revision of the contribution to the ${}^7\text{Li}$ abundance from GCR spallation too could be needed.

Appendix

Star by star analysis

In order to identify the stars which can be actually considered as tracers of the upper envelope at every metallicity, and discard the depleted ones, we analysed in detail the abundances of all the stars defining the upper envelope in the A(Li) – [Fe/H] diagram for metallicities larger than ~ -1.5 dex. The stars are listed below in order of metallicity.

- 1– HIP 42887: Deliyannis et al. (1990) give $A(\text{Li}) \leq 2.50$ and $[\text{Fe}/\text{H}] = -1.30$; Glaspey et al. (1994) reduce this upper limit to $A(\text{Li}) < 1.20$ and assume $[\text{Fe}/\text{H}] = -1.22$. Since these are only upper limits for the Li abundance in this star, we do not take this object into account as a tracer of the upper envelope.
- 2– HIP 99423: we assume $A(\text{Li}) = 2.34$ and $[\text{Fe}/\text{H}] = -1.53$ for this star (averaging on three measures, see Tab.4).
- 3– HIP 3026: only one Li detection ($A(\text{Li}) = 2.35$, $[\text{Fe}/\text{H}] = -1.20$).
- 4– HIP 86321: two A(Li) determinations in substantial agreement (from the compilation of Deliyannis et al., 1990). We took their average value: $A(\text{Li}) = 2.27$. For the metallicity we preferred the value -1.00 , according with the estimate in Cayrel de Strobel et al. (1992).
- 5– HIP 108490: we listed three ${}^7\text{Li}$ determinations for this star in Tab.4. They differ by $0.1-0.2$ dex, the mean value being 2.30. This estimate agrees with the most recent determination of the atmospheric lithium abundance in this star by Stephens et al. (1997) ($A(\text{Li}) = 2.39$).
- 6– HIP 79720 ($A(\text{Li}) = 2.40$, $[\text{Fe}/\text{H}] = -0.73$) and HIP 29001 ($A(\text{Li}) = 2.48$, $[\text{Fe}/\text{H}] = -0.71$). For these two crucial objects we found a Li detection only by Lambert et al. (1991), and an independent confirmation is desirable considering their importance in the economy of the discussion.
- 7– The Li I feature in the atmosphere of HIP 112935 is given as $W(\text{Li}) = 47 \text{ m}\text{\AA}$ by Deliyannis et al. (1990), referring to the detection by Duncan (1981), whereas Balachandran (1990) gives less than $1 \text{ m}\text{\AA}$ ($A(\text{Li}) < 0.82$). Moreover, both the Lambert et al. (1991) and Boesgaard et al. (1998) estimates ($A(\text{Li}) < 1.28$ and $A(\text{Li}) \leq 0.90$, respectively) agree with the Balachandran one. These upper limits and the detection by Duncan are not consistent; we choose the upper limit as the correct indicator of the ${}^7\text{Li}$ content in HIP 112935.
- 8– HIP 14181 ($A(\text{Li}) = 2.31$ and $[\text{Fe}/\text{H}] = -0.62$) and HIP 21167 ($A(\text{Li}) = 2.34$ and $[\text{Fe}/\text{H}] = -0.61$), both single detections from Lambert et al. (1991).
- 9– At $[\text{Fe}/\text{H}] \sim -0.5$ there are some stars lying around $A(\text{Li}) \sim 2.40$, then a steep rise occurs at $[\text{Fe}/\text{H}] \sim -0.3$: HIP 10306, HIP 11783 and HIP 46853 show that the ISM Li abundance rapidly increases to $\sim 3.2-3.3$.

Acknowledgements. It is a pleasure to thank F. D’Antona for useful discussions about nova systems and AGB stars evolution, M. Della Valle for explanations concerning the observed nova outburst rate in the Galaxy at the present time and J. Danziger for useful comments during the course of this work. We also thank E. Casuso and J. Beckman for providing us with a copy of their paper prior to publication. Finally, we would like to thank an anonymous referee for his/her useful suggestions.

This research has made use of the SIMBAD data-base, operated at CDS, Strasbourg, France, of the HIPPARCOS catalogue and of NASA’s Astrophysics Data System Abstract Service.

Table 3. Data sample. Kinematics and evolutionary status.

HD	DM	G	HIP	U	V	W	σ_U	σ_V	σ_W	kin.	ev. s.
HD 400	BD+35 8		HIP 699	-27.	-9.	-9.	4.	8.	4.	disk	to
HD 693	BD-16 17		HIP 910	-19.	-13.	-18.	0.	3.	10.	disk	to
HD 1581	CPD-65 13		HIP 1599	73.	-4.	-43.	4.	5.	8.	disk	to
HD 2454	BD+09 47		HIP 2235	-13.	-31.	-14.	3.	6.	8.	disk	to
HD 3567	BD-09 122	G 270-23	HIP 3026	-137.	-236.	-42.	19.	32.	16.	halo	to
HD 3823	CD-60 118		HIP 3170	113.	-18.	-33.	3.	4.	8.	disk	to
HD 4614	BD+57 150		HIP 3821	30.	-10.	-17.	5.	8.	1.	disk	to
HD 4813	BD-11 153		HIP 3909	-21.	-3.	-12.	2.	2.	10.	disk	to
HD 5015	BD+60 124		HIP 4151	6.	21.	14.	6.	8.	0.	disk	to
HD 6920	BD+41 219		HIP 5493	-35.	8.	-9.	6.	7.	4.	disk	to
HD 7439	BD-08 216		HIP 5799	34.	22.	-8.	3.	2.	9.	disk	to
HD 7476	BD-01 162		HIP 5833	27.	42.	-4.	3.	3.	9.	disk	to
HD 9826	BD+40 332		HIP 7513	-28.	-22.	-15.	6.	7.	3.	disk	to
	BD+72 94	G 245-32	HIP 8314	-307.	-114.	28.	30.	20.	16.	halo	to
HD 11112	CD-42 638		HIP 8398	89.	-43.	-21.	3.	3.	9.	disk	to
HD 13555	BD+20 348		HIP 10306	20.	-12.	4.	7.	4.	6.	disk	to
HD 14802	CD-24 1038		HIP 11072	19.	-17.	-10.	3.	2.	9.	disk	to
HD 15335	BD+29 423		HIP 11548	25.	32.	-14.	7.	5.	5.	disk	to
HD 15798	BD-15 449		HIP 11783	-31.	-4.	18.	4.	1.	9.	disk	to
HD 16031	BD-13 482		HIP 11952	-11.	-101.	-71.	10.	20.	9.	?	to
HD 16895	BD+48 746		HIP 12777	31.	1.	-1.	8.	6.	2.	disk	to
HD 17051	CD-51 641		HIP 12653	31.	-17.	-7.	0.	5.	9.	disk	to
HD 18768	BD+46 678		HIP 14181								to
HD 20407	CD-46 968		HIP 15131	6.	16.	-14.	1.	5.	8.	disk	to
HD 20807	CPD-62 265		HIP 15371	70.	-47.	17.	1.	7.	7.	disk	to
HD 22484	BD-00 572		HIP 16852	-1.	-15.	-42.	8.	1.	7.	disk	to
HD 22879	BD-03 592	G 80-15	HIP 17147	105.	-86.	-40.	7.	2.	7.	disk	to
HD 26491	CD-64 143		HIP 19233	39.	-27.	-16.	1.	7.	7.	disk	to
HD 284248	BD+21 607	G 8-16	HIP 19797	353.	-147.	-76.	10.	19.	5.	halo	to
HD 28620	BD+36 907		HIP 21167	4.	-4.	3.	10.	3.	1.	disk	to
HD 30495	BD-17 954		HIP 22263	21.	-6.	0.	7.	5.	6.	disk	to
HD 30649	BD+45 992	G 81-38	HIP 22596	57.	-81.	-9.	9.	5.	0.	disk	to
HD 32778	CD-56 1071		HIP 23437	76.	13.	-11.	1.	8.	6.	disk	to
HD 33256	BD-04 1056		HIP 23941	9.	-6.	3.	8.	4.	4.	disk	to
HD 34328	CD-59 1024		HIP 24316	206.	-350.	100.	14.	14.	17.	halo	to
HD 34721	BD-18 1051		HIP 24786	36.	-44.	21.	7.	6.	5.	disk	to
HD 37655	CD-43 1954		HIP 26488	86.	-22.	22.	4.	8.	5.	disk	to
HD 39587	BD+20 1162		HIP 27913	-14.	2.	-7.	10.	2.	0.	disk	to
HD 41330	BD+35 1334		HIP 28908	-6.	-25.	-33.	10.	1.	1.	disk	to
HD 41640	BD+16 1001		HIP 29001								to
HD 43042	BD+19 1270		HIP 29650	33.	-19.	-16.	10.	2.	0.	disk	to
HD 43947	BD+16 1091		HIP 30067	39.	-11.	-2.	10.	3.	0.	disk	to
HD 48938	CD-27 3248		HIP 32322	24.	26.	17.	5.	8.	2.	disk	to
HD 51530	BD+26 1405		HIP 33595	18.	31.	-22.	10.	2.	3.	disk	to
HD 53705	CD-43 2906		HIP 34065	52.	-73.	-20.	3.	9.	3.	disk	to
HD 55575	BD+47 1419		HIP 35136	80.	-2.	33.	9.	1.	4.	disk	to
HD 58551	BD+21 1596		HIP 36152	60.	-4.	-27.	9.	3.	3.	disk	to
		G 90-3	HIP 36430								sg
HD 59984	BD-08 1964		HIP 36640	29.	-51.	-18.	7.	7.	1.	disk	to
HD 61421	BD+05 1739		HIP 37279	-5.	-9.	-19.	8.	5.	2.	disk	to
HD 62407	BD+13 1750		HIP 37723	23.	-27.	-17.	8.	6.	7.	disk	sg

HD 62301	BD+39 1998		HIP 37789	7.	-109.	-22.	9.	4.	5.	?	to
HD 63077	CD-33 4113		HIP 37853	145.	-59.	41.	4.	9.	1.	?	to
HD 65907	CD-59 1773		HIP 38908	-12.	-23.	34.	1.	10.	3.	disk	to
HD 67458	CD-29 5555		HIP 39710	-61.	-6.	10.	4.	9.	0.	disk	to
HD 69897	BD+27 1589		HIP 40843	24.	-39.	7.	8.	2.	5.	disk	to
HD 73524	CD-39 4574		HIP 42291	27.	6.	-29.	2.	10.	0.	disk	to
HD 74000	BD-15 2546		HIP 42592	-249.	-359.	58.	63.	35.	3.	halo	to
HD 74011	BD+34 1885	G 115-19	HIP 42734	28.	-70.	24.	8.	3.	6.	disk	to
	BD+25 1981	G 40-34	HIP 42887	43.	-247.	-94.	8.	51.	28.	halo	to
HD 76932	BD-15 2656		HIP 44075	47.	-92.	71.	4.	8.	3.	disk	to
HD 79028	BD+62 1058		HIP 45333	-8.	-7.	-9.	7.	3.	7.	disk	to
HD 82328	BD+52 1401		HIP 46853	57.	-35.	-24.	7.	2.	7.	disk	to
HD 86560	BD+53 1378		HIP 49070								to
HD 91347	BD+49 1966	G 196-33	HIP 51700	-50.	28.	-3.	5.	2.	8.	disk	to
HD 91752	BD+37 2100		HIP 51914	-20.	-4.	-16.	5.	1.	9.	disk	to
HD 91889	BD-11 2918		HIP 51933	-68.	-35.	-36.	2.	8.	6.	disk	to
HD 94028	BD+21 2247	G 58-25	HIP 53070	33.	-140.	8.	4.	8.	9.	halo	to
HD 95241	BD+43 2068		HIP 53791	11.	-33.	-10.	4.	1.	9.	disk	to
HD 97916	BD+02 2406		HIP 55022	-108.	11.	89.	18.	8.	11.	?	to
HD 98991	BD-17 3367		HIP 55598	52.	-35.	-18.	2.	8.	6.	disk	to
HD 99747	BD+62 1183		HIP 56035	19.	21.	-31.	5.	4.	8.	disk	to
HD 102634	BD+00 2843		HIP 57629	29.	-16.	-4.	1.	5.	9.	disk	to
HD 103799	BD+41 2253		HIP 58287	32.	-25.	21.	3.	1.	10.	disk	to
HD 106516	BD-09 3468		HIP 59750	-54.	-74.	-59.	2.	6.	8.	disk	to
HD 107113	BD+87 107		HIP 59879	-37.	14.	4.	5.	7.	5.	disk	to
HD 108134	BD+61 1294		HIP 60588	-41.	-6.	-35.	4.	4.	8.	disk	to
HD 108177	BD+02 2538	G 13-35	HIP 60632	-111.	-228.	51.	10.	19.	14.	halo	to
HD 109358	BD+42 2321		HIP 61317	31.	-4.	2.	2.	2.	10.	disk	to
HD 110897	BD+40 2570		HIP 62207	41.	7.	76.	1.	2.	10.	disk	to
HD 114762	BD+18 2700	G 63-9	HIP 64426	82.	-70.	59.	6.	4.	10.	disk	to
HD 120162	BD+69 717		HIP 67109								to
HD 121560	BD+14 2680		HIP 68030	30.	-20.	-3.	4.	0.	9.	disk	to
HD 123710	BD+75 526		HIP 68796	36.	-8.	1.	3.	7.	7.	disk	to
HD 126512	BD+21 2649	G 166-25	HIP 70520	-85.	-84.	-79.	5.	3.	9.	disk	to
HD 128167	BD+30 2536		HIP 71284	-2.	16.	-5.	3.	3.	9.	disk	to
HD 131117	CD-30 11780		HIP 72772	59.	-36.	11.	8.	4.	4.	disk	to
HD 134169	BD+04 2969		HIP 74079	-3.	-3.	-1.	7.	1.	8.	disk	sg-to
		G 152-35	HIP 76059								
HD 141004	BD+07 3023		HIP 77257	49.	-24.	-39.	7.	2.	7.	disk	to
HD 142373	BD+42 2648		HIP 77760	42.	11.	-67.	2.	6.	8.	disk	to
HD 142860	BD+16 2849		HIP 78072	-56.	-33.	-25.	6.	3.	7.	disk	to
HD 143761	BD+33 2663		HIP 78459	-55.	-35.	21.	4.	5.	7.	disk	to
	BD+42 2667	G 180-24	HIP 78640	-109.	-268.	-28.	21.	25.	14.	halo	to
HD 146588	BD+19 3076		HIP 79720								to
HD 148816	BD+04 3195	G 17-21	HIP 80837	-83.	-264.	-81.	9.	10.	6.	halo	to
HD 150453	BD-19 4406		HIP 81754	-5.	10.	2.	10.	1.	3.	disk	to
HD 155358	BD+33 2840		HIP 83949								to
HD 157089	BD+01 3421		HIP 84905	167.	-42.	-9.	9.	4.	4.	halo	to
HD 159332	BD+19 3354		HIP 85912	28.	-48.	-26.	7.	6.	4.	disk	to
HD 160291	BD+48 2541		HIP 86173	-34.	8.	-25.	3.	8.	6.	disk	to
	BD+18 3423	G 170-56	HIP 86321	83.	-265.	-50.	15.	20.	9.	halo	to
HD 160693	BD+37 2926	G 182-19	HIP 86431	-209.	-112.	85.	9.	10.	6.	halo	to
HD 160617	CD-40 11755		HIP 86694	-59.	-216.	-94.	12.	29.	12.	halo	sg
	BD-08 4501	G 20-15	HIP 87062	-141.	-49.	-163.	15.	17.	38.	halo	to

HD 165908	BD+30 3128		HIP 88745	6.	1.	10.	5.	8.	4.	disk	to
HD 166913	CD-59 6824		HIP 89554	45.	-48.	69.	9.	6.	5.	disk	to
HD 167588	BD+29 3213		HIP 89408	-41.	-17.	-17.	5.	8.	3.	disk	to
HD 168151	BD+64 1252		HIP 89348	6.	-13.	-51.	1.	9.	5.	disk	to
HD 170153	BD+72 839		HIP 89937	-3.	40.	-3.	2.	9.	5.	disk	to
HD 174912	BD+38 3327	G 207-5	HIP 92532	22.	8.	-42.	4.	9.	3.	disk	to
HD 181743	CD-45 13178		HIP 95333	47.	-334.	-60.	13.	52.	9.	halo	to
HD 186379	BD+24 3849		HIP 97023	-32.	-27.	-46.	5.	9.	2.	disk	to
HD 187691	BD+10 4073		HIP 97675	3.	-3.	-25.	6.	8.	2.	disk	to
		G 24-3	HIP 98989								to
HD 345957	BD+23 3912		HIP 99423								to
HD 194598	BD+09 4529	G 24-15	HIP 100792	74.	-276.	-30.	7.	10.	7.	halo	to
HD 195633	BD+06 4557		HIP 101346	35.	8.	-24.	7.	8.	5.	disk	sg-to
HD 199288	CD-44 14214		HIP 103458	-22.	-101.	46.	8.	2.	7.	disk	to
HD 199960	BD-05 5433		HIP 103682	7.	-24.	-3.	6.	6.	5.	disk	to
HD 200580	BD+02 4295	G 25-15	HIP 103987	-96.	-75.	9.	9.	9.	5.	disk	sg
HD 201891	BD+17 4519		HIP 104659	-92.	-115.	-59.	5.	9.	4.	?	to
HD 202628	CD-43 14464		HIP 105184	12.	2.	-27.	7.	0.	7.	disk	to
HD 203454	BD+39 4529		HIP 105406	-20.	-2.	-17.	1.	10.	1.	disk	to
HD 205650	CD-28 17381		HIP 106749	118.	-83.	11.	7.	5.	9.	disk	to
HD 207129	CD-47 13928		HIP 107649	13.	-22.	1.	6.	1.	8.	disk	to
HD 207978	BD+28 4215		HIP 107975	-13.	16.	-8.	1.	9.	3.	disk	to
HD 208906	BD+29 4550		HIP 108490	-73.	-2.	-12.	2.	9.	3.	disk	to
	BD+17 4708	G 126-62	HIP 109558	302.	-283.	11.	42.	10.	24.	halo	to
HD 210918	CD-41 14804		HIP 109821	47.	-92.	-9.	6.	1.	8.	disk	to
HD 211415	CD-54 9222		HIP 110109	30.	-41.	7.	6.	2.	8.	disk	to
	BD+07 4841	G 18-39	HIP 110140	267.	-317.	-107.	107.	74.	128.	halo	to
HD 212698	BD-17 6521		HIP 110778	19.	-6.	-5.	4.	4.	8.	disk	to
		G 18-54	HIP 111195	-11.	-267.	51.	15.	32.	24.	halo	to
HD 214953	CD-47 14307		HIP 112117	-14.	-38.	-6.	5.	1.	9.	disk	to
HD 216385	BD+09 5122		HIP 112935	58.	-7.	-33.	2.	7.	7.	disk	to
HD 218470	BD+48 3944		HIP 114210	30.	-9.	10.	3.	9.	2.	disk	to
HD 218502	BD-15 6355		HIP 114271								to
HD 219476	BD+30 4912		HIP 114838								to
HD 219623	BD+52 3410		HIP 114924	-7.	-27.	-22.	3.	9.	1.	disk	to
HD 219617	BD-14 6437	G 273-1	HIP 114962	-383.	-329.	-58.	76.	67.	13.	halo	to
	BD+02 4651	G 29-23	HIP 115167	299.	-453.	-60.	192.	206.	172.	halo	sg
	BD+59 2723	G 217-8	HIP 115704	180.	-186.	-55.	36.	18.	9.	halo	to
HD 221377	BD+51 3630		HIP 116082								sg
HD 222368	BD+04 5035		HIP 116771	8.	-27.	-26.	0.	6.	8.	disk	to

Table 4. Data sample. Effective temperatures, gravities, metallicities and lithium abundances as taken from the literature. The metallicities given in the brackets are those derived from the photometry, all the others refer to spectroscopic determinations. References: 1 = Deliyannis et al. , 1990 (their SS); 2 = Deliyannis et al. , 1990 (their HD); 3 = Deliyannis et al. , 1990 (their RMB); 4 = Lambert et al. , 1991; 5 = Pilachowski et al. , 1993; 6 = Pasquini et al. , 1994; 7 = Spite et al. , 1996 (in this paper the temperature has been determined from either the excitation balance of the FeI lines or the dereddened $(b - y)_0$ color or the profile of the H_α wings. The gravity has been estimated from the position in the $c_1 - (b - y)_0$ diagram or by comparing the iron abundance deduced from FeI and FeII lines. When multiple determinations are given, we list all of them).

HIP	T_{eff}	$\log g$	[Fe/H]	W(Li)	A(Li)	upper limits	ref.
HIP 699	6190	4.13	-0.35	22	+2.18		4
HIP 910	6200	4.07	-0.38	34	+2.39		4
HIP 1599	6009	4.52	-0.26 (-0.15)	40	+2.36		6
HIP 2235	6490	4.08	-0.37	4	+1.62	u	4
HIP 3026	5950	4.00	-1.20	45	+2.35		3
HIP 3170	6037	4.34	-0.35 (-0.35)	45	+2.44		6
HIP 3821	5950	4.47	-0.31	21	+1.98		4
HIP 3909	6250	4.32	-0.15	64	+2.77		4
HIP 4151	6200	3.98	+0.00	2	+1.10	u	4
HIP 5493	5800	3.88	-0.21	4	+1.13	u	4
HIP 5799	6470	4.10	-0.32	4	+1.58		4
HIP 5833	6520	4.01	-0.24	29	+2.54		4
HIP 7513	6210	4.17	+0.09	30	+2.36		4
HIP 8314	6160	4.50	-1.80	27	+2.22		3
	6160	3.00		27.0	+2.22		5
HIP 8398	5800	4.03	-0.07 (-0.20)	57	+2.37		6
HIP 10306	6360	4.07	-0.32	64	+2.84		4
HIP 11072	5905	4.19	-0.19 (-0.07)	51	+2.40		6
HIP 11548	5860	4.06	-0.22	52	+2.34		4
HIP 11783	6440	3.94	-0.25	81	+3.03		4
HIP 11952	5929	4.00	-2.20	28.0	+2.03		1
	5970	3.90	-1.89 (-1.89)	28.0	+2.07		7
HIP 12777	6310	4.30	-0.02	67	+2.84		4
HIP 12653	6074	4.22	-0.04 (+0.01)	38	+2.39		6
HIP 14181	5720	4.04	-0.62	61	+2.31		4
HIP 15131	5879	4.32	-0.55 (-0.37)	15	+1.79		6
HIP 15371	5856	4.40	-0.38 (-0.50)	3	+0.93	u	6
HIP 16852	5980	4.15	-0.15	41	+2.33		4
HIP 17147	5740	4.10	-0.60	25	+1.80		2
HIP 19233	5744	4.19	-0.28 (-0.30)	3	+0.93	u	6
HIP 19797	5929	4.00	-1.60	25.0	+1.98		1
HIP 21167	6140	4.06	(-0.61)	34	+2.34		4
HIP 22263	5829	4.30	-0.13 (+0.01)	56	+2.39		6
HIP 22596	5700	4.10	-0.30	33	+1.90		2
	5740	4.22	-0.51	2	+0.76	u	4
HIP 23437	5760	4.34	-0.61 (-0.30)	8	+1.40		6
HIP 23941	6440	4.05	-0.30	3	+1.43	u	4
HIP 24316	5730	4.60	-1.60 (-1.60)	32.0	+1.98		7
HIP 24786	6001	4.09	-0.25 (-0.18)	39	+2.35		6
HIP 26488	5874	4.04	-0.31 (-0.31)	46	+2.32		6
HIP 27913	5950	4.46	-0.03	95	+2.77		4
HIP 28908	5920	4.14	-0.24	19	+1.89		4
HIP 29001	6080	4.33	(-0.71)	49	+2.48		4
HIP 29650	6590	4.27	+0.04	6	+1.86		4
HIP 30067	5950	4.28	-0.30	38	+2.25		4
HIP 32322	6018	4.30	-0.56 (-0.59)	33	+2.27		6
HIP 33595	6020	3.94	-0.56	3	+1.16	u	4
HIP 34065	5812	4.33	-0.36 (-0.26)	3	+0.98	u	6

HIP 35136	5960	4.48	-0.28	10	+1.62		4
HIP 36152	6180	4.17	-0.55	36	+2.40		4
HIP 36430	5900	3.00	-1.93	43.5	+2.25		5
HIP 36640	5980	4.18	-0.74	43	+2.33		4
HIP 37279	6700	4.03	-0.02	2	+1.48	u	4
HIP 37723	5820	4.26	(-0.71)	18	+1.78		4
HIP 37789	5900	4.19	-0.69	27	+2.03		4
HIP 37853	5778	4.27	-0.90 (-0.78)	8	+1.41		6
HIP 38908	6072	4.50	-0.36 (-0.20)	3	+1.20	u	6
HIP 39710	5962	4.47	-0.24 (-0.06)	26	+2.12		6
HIP 40843	6360	4.35	-0.26	52	+2.73		4
HIP 42291	5972	4.32	-0.01 (+0.06)	46	+2.41		6
HIP 42592	6223	4.50	-1.80	24.5	+2.16		1
HIP 42734	5740	4.15	-0.65	16	+1.69		4
HIP 42887	6780	4.10	-1.30	12	+2.50	u	2
HIP 44075	5861	3.50	-1.10	23.0	+1.96		1
	5970	4.37	-0.82	24	+2.05		4
	5900	3.00	-0.90	26.7	+2.02		5
HIP 45333	5880	4.18	-0.08	11	+1.63		4
HIP 46853	6380	4.09	-0.20	102	+3.15		4
HIP 49070	5910	4.13	(-0.59)	28	+2.07		4
HIP 51700	5870	4.24	-0.48	21	+1.91		4
HIP 51914	6490	3.92	-0.23	2	+1.33	u	4
HIP 51933	6140	4.22	-0.24	38	+2.41		4
HIP 53070	5794	4.00	-1.70	35.0	+2.09		1
	5860	4.10	-1.70	33	+2.10		2
	5800	3.00	-1.51	36.6	+2.09		5
HIP 53791	5890	4.05	-0.30	1	+0.35	u	4
HIP 55022	6124	4.00	-1.10	3.0	+1.20	u	1
	6000	3.00	-1.38	5.0	+1.30	u	5
HIP 55598	6640	3.98	-0.11	3	+1.63	u	4
HIP 56035	6610	3.99	-0.54	5	+1.80	u	4
HIP 57629	6390	4.18	+0.24	33	+2.53		4
HIP 58287	6220	4.04	(-0.43)	19	+2.13		4
HIP 59750	6067	4.30	-0.40	11.0	+1.80	u	1
	6110	4.10	-0.90	6	+1.50	u	2
	6250	4.38	-0.70	3	+1.32	u	4
HIP 59879	6390	4.07	-0.54	4	+1.55	u	4
HIP 60588	5830	4.21	(-0.58)	20	+1.85		4
HIP 60632	5847	4.50	-1.90	35.0	+2.09		1
	5900	4.10	-1.90	24	+1.90	u	2
	5861		-1.90	29	+2.00		3
HIP 61317	5880	4.52	-0.19	9	+1.53		4
HIP 62207	5794	3.90	-0.30	33.0	+2.10		1
	5800	4.15	-0.59	20	+1.82		4
HIP 64426	5750	4.10	-0.80	17	+1.60		2
	5740	4.00	-0.80	25	+1.88		3
	5870	4.24	-0.74	22	+1.92		4
HIP 67109	5900	4.38	(-0.80)	31	+2.11		4
HIP 68030	6190	4.36	(-0.37)	38	+2.44		4
HIP 68796	5740	4.00	-0.60	23	+1.85		3
HIP 70520	5750	4.20	-0.63	16	+1.69		4
HIP 71284	6770	4.27	-0.41	3	+1.67	u	4
HIP 72772	6000	4.09	+0.13	66	+2.60		4

HIP 74079	5794	3.80	-1.60	44.0	+2.23	1
	5800	4.10	-1.60	46	+2.20	2
	5800	3.00		44.0	+2.18	5
HIP 76059	5600, 5700	4.50, 3.80	-1.75 (-1.61)	53.7	+2.13, +2.21	7
HIP 77257	5940	4.21	-0.04	20	+1.95	4
HIP 77760	5794	3.90	-0.30	69.0	+2.58	1
	5830	4.10	-0.40	56	+2.40	2
	5840	4.34	-0.52	49	+2.30	4
HIP 78072	6330	4.25	-0.16	17	+2.15	4
HIP 78459	5780	4.24	-0.26	6	+1.28	4
HIP 78640	5960	4.00	-1.70	28	+2.12	3
HIP 79720	5980	4.33	(-0.73)	38	+2.40	4
HIP 80837	5534	4.00	-0.50	17.0	+1.53	1
	5810	4.10	-0.70	18	+1.70	2
HIP 81754	6440	3.86	-0.31	29	+2.49	4
	5870	4.19	-0.67	20	+1.87	4
HIP 84905	5861	3.70	-0.50	25.0	+2.11	1
	5735	4.10	-0.60	20	+1.70	2
HIP 85912	6240	3.91	-0.23	4	+1.45	u 4
	6070	4.19	(-0.61)	25	+2.14	4
HIP 86173	6070	4.19	(-0.61)	25	+2.14	4
	6067	4.00	-1.00	31.0	+2.19	1
HIP 86321	6140	4.00	-0.80	34	+2.35	3
	5780	4.10	-0.70	7	+1.20	u 2
HIP 86431	5710	4.00	-0.70	4	+1.00	u 3
	5861	3.50	-1.60	42.0	+2.20	1
HIP 86694	5900	3.00		42.0	+2.23	5
	5600	3.00	-1.78	28.3	+1.80	5
HIP 87062	5830, 5900	4.00, 4.00	-1.40 (-1.58)	35.1	+2.09, +2.14	7
	5998	4.20	-0.40	41.0	+2.38	1
HIP 88745	6020	4.48	-0.56	34	+2.25	4
	5861	3.30	-1.80	40.0	+2.17	1
HIP 89554	5900	4.23	(-0.38)	41	+2.26	4
HIP 89408	5900	4.23	(-0.38)	41	+2.26	4
HIP 89348	6590	4.09	-0.32	2	+1.40	u 4
HIP 89937	6152	4.30	-0.30	42.0	+2.52	1
	5920	4.10	-0.30	29	+2.00	2
HIP 92532	5860	4.33	-0.54	29	+2.05	4
	5790, 5900	4.50, 3.50	-1.70 (-1.89)	40.6	+2.13, +2.21	7
HIP 95333	5880	4.11	(-0.55)	40	+2.22	4
HIP 97023	6150	4.14	+0.09	63	+2.69	4
HIP 97675	6150	4.14	+0.09	63	+2.69	4
HIP 98989	5800		-1.63	28.5	+1.97	5
HIP 99423	5596	4.00	-1.70	67.0	+2.23	1
	5720	4.00	-1.30	73	+2.40	3
	5600	3.00	-1.59	80.8	+2.38	5
HIP 100792	5808	4.00	-1.60	29.0	+2.00	1
HIP 101346	5840	3.80	-0.90	40	+2.15	3
HIP 103458	5727	4.35	-0.82 (-0.64)	3	+0.86	u 6
HIP 103682	5810	4.20	+0.11	53	+2.32	4
HIP 103987	5730	3.50	-0.70	32	+2.00	3
HIP 104659	5794	4.50	-1.40	23.0	+1.89	1
	5810	4.10	-1.40	27	+1.90	2
	5850	4.50	-1.00	27	+2.08	3
	5870	4.46	-1.06	21	+1.90	4
HIP 105184	5771	4.52	-0.14	41	+2.17	6
HIP 105406	5750	4.10	-0.30	64	+2.40	2

HIP 106749	5728	4.00	-1.30	18.0	+1.67		1
HIP 107649	5948	4.13	-0.15 (-0.05)	38	+2.29		6
HIP 107975	5780	4.10	-0.50	5	+1.10	u	2
HIP 108490	5900	4.10	-0.50	43	+2.20		2
	5960	4.00	-0.90	50	+2.40		3
	6010	4.41	-0.72	38	+2.30		4
HIP 109558	5810	4.10	-2.00	25	+1.90		2
	5890	4.00	-1.70	25	+1.98		3
HIP 109821	5802	4.43	-0.18 (+0.10)	3	+0.94	u	6
HIP 110109	5870	4.35	-0.36 (-0.32)	10	+1.60		6
HIP 110140	5920	4.00	-1.20	37	+2.24		3
HIP 110778	5915	4.50	-0.13 (-0.14)	114	+2.89		6
HIP 111195	5800	3.00	-1.33	34.9	+2.07		5
HIP 112117	6069	4.49	-0.09 (+0.07)	65	+2.67		6
HIP 112935	6067	3.90	-0.62	47.0	+2.53		1
	6290	3.97	-0.25	2	+1.28	u	4
HIP 114210	6600	4.21	-0.13	4	+1.72	u	4
HIP 114271	6000	3.00	-1.96	30.0	+2.16		5
HIP 114838	5930	4.01	(-0.68)	2	+0.91	u	4
HIP 114924	6130	4.21	+0.00	64	+2.68		4
HIP 114962	5662	3.90	-1.40	42.0	+2.04		1
	5820	4.10	-1.40	43	+2.20		2
	5870	4.50	-1.50	40	+2.20		3
HIP 115167	5794	4.00	-2.30	27.0	+1.92		1
HIP 115704	5830	4.00	-1.60	25	+1.95		3
HIP 116082	6000	3.50	-1.10	6	+1.45	u	3
	6320	3.89	(-0.72)	3	+1.41	u	4
HIP 116771	5998	3.90	-0.50	22.0	+2.05		1
	6260	4.16	-0.17	18	+2.14		4

References

- Abia, C., Boffin, H.M.J., Isern, J., Rebolo, R. 1991, *A&A* 245, L1
- Abia, C., Boffin, H.M.J., Isern, J., Rebolo, R. 1993a, *A&A* 272, 455
- Abia, C., Isern, J., Canal, R. 1993b, *A&A* 275, 96
- Abia, C., Isern, J., Canal, R. 1995, *A&A* 298, 465
- Allen, C.W. 1954, *MNRAS* 114, 387
- Alonso, A., Arribas, S., Martinez-Roger, C. 1996, *A&A* 313, 873
- Anders, E., Grevesse, N. 1989, *Geochim. Cosmochim. Acta* 53, 197
- Balachandran, S. 1990, *ApJ* 354, 310
- Bath, G.T., Shaviv, G. 1978, *MNRAS* 183, 515
- Beers, T.C., Preston, G.W., Shectman, S.A. 1992, *AJ* 103, 1987
- Beers, T.C., Preston, G.W., Shectman, S.A., Kage, J.A. 1990, *AJ* 100, 849
- Beers, T.B., Sommer-Larsen, J. 1995, *ApJSupp* 96, 175
- Bertelli, G., Bressan, A., Chiosi, C., Fagotto, F., Nasi, E. 1994, *A&ASupp* 106, 275
- Boesgaard, A.M., Deliyannis, C.P., Stephens, A., Lambert, D.L. 1998, *ApJ* 492, 727
- Boffin, H.M.J., Paulus, G., Arnould, M., Mowlavi, N. 1993, *A&A* 279, 173
- Bonifacio, P., Centurion, M., Molaro, P. 1999, *MNRAS*, in press
- Bonifacio, P., Molaro, P. 1997, *MNRAS* 285, 847
- Cameron, A.G.W., Fowler, W.A. 1971, *ApJ* 164, 111
- Cayrel, R., Spite, M., Spite, F., Vangioni-Flam, E., Cassé, M., Audouze, J. 1999, *A&A* 343, 923
- Cayrel de Strobel, G., Hauck, B., François, P., Thévenin, F., Friel, E., Mermilliod, M., Borde, S. 1992, *A&ASupp* 95, 273
- Chamcham, K. 1998, private communication
- Chiappini, C., Matteucci, F., Gratton, R. 1997, *ApJ* 477, 765
- Chiosi, C., Bertelli, G., Bressan, A. 1992, *Ann. Rev. A&A* 30, 235
- Ciardullo, R., Ford, H.C., Williams, R.E., Tamblyn, P., Jacoby, G.H. 1990, *AJ* 99, 1079
- D'Antona, F., 1998, private communication
- D'Antona, F., Matteucci, F. 1991, *A&A* 247, L37
- Deliyannis, C.P., Demarque, P., Kawaler, S.D. 1990, *ApJSupp* 73, 21
- Della Valle, M., Livio, M. 1994, *A&A* 286, 786
- Duncan, D.K. 1981, *AJ* 248, 651
- Duncan, D.K., Primas, F., Rebull, L.M., Boesgaard, A.M., Deliyannis, C.P., Hobbs, L.M., King, J.R., Ryan, S.G. 1997, *ApJ* 488, 338
- Duncan, D.K., Rebull, L.M. 1996, *PASP* 108, 738
- Fields, B.D., Olive, K.A. 1999, *New Astronomy* 4, 255
- García López, R.J., Lambert, D.L., Edvardsson, B., Gustafsson, B., Kiselman, D., Rebolo, R. 1998, *ApJ* 500, 241
- Gehrz, R.D., Truran, J.W., Williams, R.E., Starrfield, S. 1998, *PASP* 110, 3
- Glaspey, J.W., Pritchett, C.J., Stetson, P.B. 1994, *AJ* 108, 271
- Hatano, K., Branch, D., Fisher, A., Starrfield, S. 1997, *MNRAS* 290, 113
- Hernanz, M., José, J., Coc, A., Isern, J. 1996, *ApJ* 465, L27
- Hobbs, L.M., Thorburn, J.A. 1997, *ApJ* 491, 772
- Iben, I.Jr. 1973, *ApJ* 185, 209
- Johnson, D.R.H., Soderblom, D.R. 1987, *AJ* 93, 864
- José, J., Hernanz, M. 1998, *ApJ* 494, 680
- Kopylov, I.M. 1955, *Izv. Krymskoi Astrofiz. Obs.* 13, 23
- Lambert, D.L., Heath, J.E., Edvardsson, B. 1991, *MNRAS* 253, 610
- Lemoine, M., Ferlet, R., Vidal-Madjar, A. 1995, *A&A* 298, 879
- Lemoine, M., Vangioni-Flam, E., Cassé, M. 1998, *ApJ* 499, 735
- Liller, W., Mayer, B. 1987, *PASP* 99, 606
- Livio, M. 1994, in *Interacting Binaries*, ed. H. Nussbaumer & A. Orr (Berlin, Springer), 135
- Marigo, P., Bressan, A., Chiosi, C. 1996, *A&A* 313, 545
- Matteucci, F., D'Antona, F., Timmes, F.X. 1995, *A&A* 303, 460
- Matteucci, F., Romano, D., Molaro, P. 1999, *A&A* 341, 458
- Mazzitelli, I., D'Antona, F., Ventura, P., Zeppieri, A. 1999 in *Theory and tests of convective energy transport*, *PASP*, in press
- Molaro, P., Bonifacio, P., Castelli, F., Pasquini, L. 1997, *A&A* 319, 593
- Norris, J.E., Ryan, S.G., Beers, T.C. 1997, *ApJ* 488, 350
- Pasquini, L., Liu, Q., Pallavicini, R. 1994, *A&A* 287, 191
- Pilachowski, C.A., Sneden, C., Booth, J. 1993, *ApJ* 407, 699
- Pinsonneault, M.H., Deliyannis, C.P., Demarque, P. 1992, *ApJSupp* 78, 179
- Plez, B., Smith, V.V., Lambert, D.L. 1993, *ApJ* 418, 812
- Rebolo, R., Molaro, P., Beckman, J.E. 1988, *A&A* 192, 192 (RMB)
- Ryan, S.G., Deliyannis, C.P. 1998, *ApJ* 500, 398
- Ryan, S.G., Norris, J.E., Beers, T.C. 1999, *ApJ* submitted
- Sackmann, I.J., Boothroyd, A.I. 1992, *ApJ* 392, L71
- Sandage, A., Fouts, G. 1987, *AJ* 93, 74
- Shafter, A.W. 1997, *ApJ* 487, 226
- Shara, M.M., Livio, M., Moffat, A.F.J., Orio, M. 1986, *ApJ* 311, 163
- Sharov, A.S. 1972, *Soviet Astron.* 16, 41
- Smith, V.V., Lambert, D.L. 1990, *ApJ* 361, L69
- Smith, V.V., Lambert, D.L., Nissen, P.E. 1993, *ApJ* 408, 262
- Smith, V.V., Plez, B., Lambert, D.L., Lubowich, D.A. 1995, *ApJ* 441, 735
- Spite, M., François, P., Nissen, P.E., Spite, F. 1996, *A&A* 307, 172
- Spite, M., Maillard, J.P., Spite, F. 1984, *A&A* 141, 56
- Spite, F., Spite, M. 1982, *A&A* 115, 357
- Spite, F., Spite, M. 1986, *A&A* 163, 140
- Starrfield, S., Truran, J.W., Sparks, W.M., Arnould, M. 1978, *ApJ* 222, 600
- Steigman, G., Walker, T.P. 1992, *ApJ* 385, L13
- Stephens, A., Boesgaard, A.M., King, J.R., Deliyannis, C.P. 1997, *ApJ* 491, 339

- Timmes, F.X., Woosley, S.E., Weaver, T.A. 1995, ApJSupp 98, 617
- Thorburn, J.A. 1994, ApJ 421, 318
- Vauclair, S. 1988, ApJ 335, 971
- Vauclair, S., Charbonnel, C. 1995, A&A 295, 715
- Wallerstein, G., Conti, P.S. 1969, Ann. Rev. A&A 7, 99
- Weidemann, V. 1967, Z. Astrophys. 67, 286
- Woosley, S.E., Hartmann, D.H., Hoffman, R.D., Haxton, W.C. 1990, ApJ 356, 272
- Woosley, S.E., Weaver, T.A. 1995, ApJSupp 101, 181
- Yuan, J.W. 1989, A&A 224, 108